J Mol Model (2013) 19:2797–2810
DOI 10.1007/s00894-012-1638-2

ORIGINAL PAPER

Computational design of a CNT carrier for a high affinity bispecific anti-HER2 antibody based on trastuzumab and pertuzumab Fabs

Karim Salazar-Salinas · Carlos Kubli-Garfias · Jorge M. Seminario

Received: 5 September 2012 / Accepted: 7 October 2012 / Published online: 10 November 2012

Abstract This is a preliminary cross multidisciplinary theoretical-computational approach for the design of a drug delivery system based on immunoconjugated carbon nanotube against HER2- overexpressing cancer cells. This drug delivery system allows the release of an encapsulated cytotoxic cocktail in a controlled manner under pulsed radio frequency (RF) irradiation. Our effort is focused on the computational aided design of a high affinity bispecific anti-HER2 antibody and an opening mechanism of the carbon nanotube (CNT) based cytotoxic carrier for controlling multiple drug release. We study the main interactions between the antibody and the antigen by a computational scanning mutagenesis approach of trastuzumab and pertuzumab fragment antigen binding (Fab) structures in order to enhance their binding affinity. Then, each Fab fragments is joined by a polypeptide linker which should be stable enough to avoid the "open form" of antibody. On the other hand, we also conjugate the engineered antibody to functionalized CNTs (*f*-CNTs), which encapsulate the inhibitors of the HER2/PI3K/Akt/mTOR signaling pathway. We take advantage of the fact that *f*-CNT converts the RF radiation absorption into heat release. A pulsed laser at 13.45 MHz increments the temperature around 40 °C for triggering the nano-caps destabilization, which allows the switching of the opening mechanism of the drug carrier. Nano-caps will be a dual pH/temperature responsive in order to take advantage of lysosome characteristic (acidic pH) and heat release from the carrier. Nano-caps are functionalized with organic amide moieties, which hydrolyze quickly at an acidic pH into primary amines, and protonated amines generate repulsion interactions with other charged species, which trigger the cytotoxics release.

Keywords Antibody · Anti-HER2 · Cytotoxic carrier · Computational · CNT · Design · Fabs · Pertuzumab · Trastuzumab

K. Salazar-Salinas · C. Kubli-Garfias · J. M. Seminario (✉)
Department of Chemical Engineering, Texas A&M University,
College Station, TX, USA
e-mail: seminario@tamu.edu

K. Salazar-Salinas · C. Kubli-Garfias · J. M. Seminario
Department of Electrical and Computer Engineering,
Texas A&M University,
College Station, TX, USA

K. Salazar-Salinas · C. Kubli-Garfias · J. M. Seminario
Materials Science and Engineering Program,
Texas A&M University,
College Station, TX, USA

C. Kubli-Garfias
Instituto de Investigaciones Biomédicas, Universidad
Nacional Autónoma de México,
México D.F., Mexico

Introduction

The relevance of cancer research to public health is direct and enormous; we need to create proficient substances able to eradicate cancer cells directly without damaging normal cells. Given the biochemical-atomistic nature of cancer, a nanotechnology theory-guided approach based on the most precise laws of nature will not only be useful to combat cancer but any other disease. On the other hand nanotechnology computational tools can help us to understand that biological events always initiate from elementary interactions between electrons and, fortunately, these events can be precisely analyzed and predicted, no matter how big they are, how large the involved populations are, or how different and complex their emergent properties are. All is just a matter of a strategic approach.

Therefore, there is a need to develop the chemistry and physic frames of a specific, direct and efficient drug delivery system against cancer cells through a path across cytotoxic, drug carrier, and radiology disciplines. The development of

those frames allows the use of functionalized carbon nanotube (*f*-CNTs) as cytotoxic carriers. Thus a drug delivery system can consist in the conjugation of *f*-CNT with an anti-HER2 antibody and an opening mechanism for the nanotube. The cytotoxics can be concealed inside the nanotube until their release when the nanotube is opened under radio frequency (RF) radiation.

A bispecific antibody based on the fragment antigen binding (Fab) from trastuzumab (against domain 4 HER2 receptor) and pertuzumab (against domain 2 HER2 receptor) represents a combined way to block the HER2 receptor activation. To design a high affinity bispecific anti-HER2-antibody, a test of how residues in the trastuzumab and pertuzumab Fab paratopes contribute to HER2 receptor binding affinity can be performed through a computational scanning mutagenesis of a wide variety of antibody-ligand complexes. Hot-spot residues can be identified through an increasing of the binding affinity by more than 2.0 kcal mol^{-1}. The adequate mutation of the bispecific anti-Her2 antibody needed to increase its binding energy can also be determined from the structure-energetic analysis. The prediction of the differences in binding free energies between the wild-type and mutated complexes $\left(\Delta\Delta G_{binding}\right)$ can be determined by a fully atomistic computational approach by molecular dynamics simulations. This is a very interesting point, since we also need to know very well the antigen surface where the paratope interacts. Besides, knowing the binding characteristics and the residues in both sides that play the role of "pharmacophores" may help to develop specific drugs acting on the receptor surface.

We have to consider that the traditional disciplines are oriented vertically and strongly specialized overlapping with some other disciplines. Nanotechnology offers new techniques and approaches to go across the above disciplines horizontally toward the development of new strategies to improve cancer therapies. In this study, we go across cytotoxic, drug carrier and radiology disciplines horizontally (Fig. 1). This approach is slightly overlapping with all the traditional ones, and uses a set of computational techniques equally valid for any biological or non-biological material. Perhaps the next practitioners in this field are not experts in the traditional sense; they just intuitively learned to use the techniques every time to new and different problems. In this work, we provide gross initial models as they may become more sophisticated as the investigation on cancer molecular biology progresses, pointing toward direct solutions of specific cancer problems.

Thus, this is an initial theoretical-computational study to design an inmunoconjugated functionalized carbon nanotube able to release the encapsulated HER2/PI3K/Akt/mTOR inhibitors under pulsed radio frequency (RF) irradiation. The functionalized carbon nanotube (*f*-CNT) is attached to a bispecific single-chain fragment variable (biscFv) able to target cancer cells, and to an opening mechanism triggered by RF radiation when the drug delivery system is internalized in the target. Consequently, chemotherapy will be extremely specific, avoiding the secondary effects of traditional chemotherapy. Thus the *f*-CNT must be attached out of the paratope region avoiding binding conflicts.

The main concern about the feasibility of the use of CNT as a drug carrier is the toxic effect of CNT. In this context several reports indicate that the cytotoxic effect of CNT is due to its agglomeration [1] and through its functionalization with polar groups like polyethyleneimine (PEI)[2–5], polyamidoamine dendrimer (PAMAM)[6] the cytotoxicity is avoided. In addition, *f*-CNT has a long circulation time in the bloodstream, it is able to bypass cellular barriers [7–12] and interact with biomolecules such as DNA [13], which shows its biocompatibility, making it a useful tool for biomedical applications such as drug vehicle [14]. The *f*-CNT has already been tested as a drug carrier for cancer therapy. It was conjugated with doxorubicin[15] and paclitaxel [16] resulting more efficient than just drugs, without inducing any toxicity [17, 18]. A recent study at the Beckman Research Institute showed that a single intracranial injection of low dose CNT-CpG eradicates intracranial GL261 gliomas

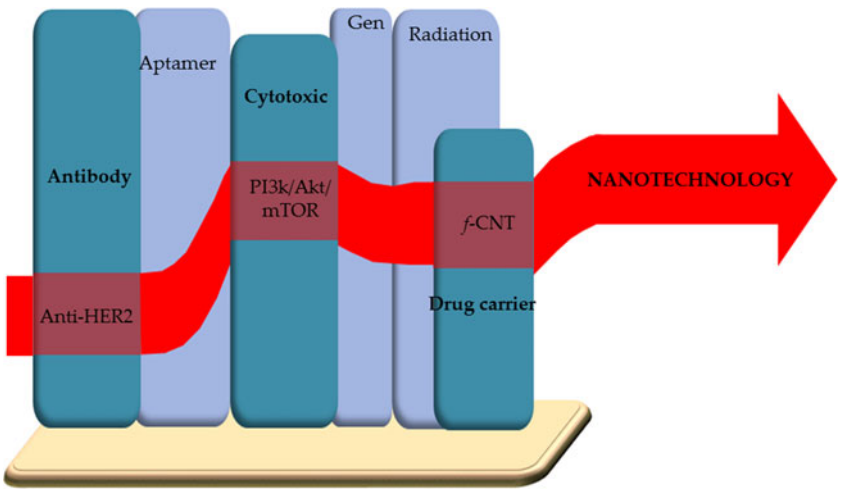

Fig. 1 Nanotechnology intersection to traditional branches toward the design of an efficient drug delivery system

in half in tumor-bearing mice [19]. Moreover, the interior of CNT could be used to safely conceal drugs or biological substances. For example, the cytotoxic carboplatin was introduced in CNT and tested successfully for the inhibition of the bladder cancer cells growth [20].

On the other hand, *f*-CNT has already been conjugated with antibodies for therapeutic and diagnostic oncology. Taking advantage of the conversion of absorbed RF into heat, the *f*-CNT can be used for selective photothermal ablation of tumors when it is attached to monoclonal antibody [21, 22]. Those findings open the door to develop new strategies for attacking malignant cells during their growth and dormant periods [23–25], and to also attack their resistance mechanisms [26, 27] by a combined treatment. In addition, these studies can also be performed on boron nitrite nanotubes (BNNT) because of their structural similarity to the CNT and noncytotoxic effects on live experimental subjects [28].

In order to develop a controllable release mechanism of inhibitors, these inhibitors need to be encapsulated in *f*-CNTs and block the HER2/PI3K/Akt/mTOR signaling pathway. They are directed toward HER2-overexpressing cancer cells through the internalization of a bispecific anti-HER2 receptor antibody attached to the *f*-CNT. The addition of an antibody to the CNT based drug carrier allows the specific infiltration of antineoplastics drugs to cancer cells. At the same time, the functionalization of CNT with polar chemical groups will increase its solubility and allow its elimination from the body, avoiding the CNT's toxicity concern, such was reported in [29].

In almost all drug delivery studies based on *f*-CNT, the cytotoxics are fixed to the CNT by covalent bond or adsorption via π-π interactions; however, guest molecules can be encapsulated into *f*-CNT, such as a protein [30], cisplatin [31], doxorubicin [32] or Pt-labelled DNA [33]. The encapsulation of drugs offers the opportunity to control their release by the design of stimuli-responsive nano-caps. pH/temperature sensible nano-caps need to be developed, which can be functionalized on the edges of the CNT. This novel drug delivery system has the benefit of creating a robust and safe structure in the bloodstream, but is sensitive to intracellular cancer cell (high concentration of superoxide compounds [34, 35], such as H_2O_2 which is up to 0.5 nmol/10^4 cell/hour [36], and acidic pH [37]).

It is very important to understand earlier to the performing of the experiments if we will be able to determine whether or not the use of targeted *f*-CNT as a drug carrier in drug delivery is safe and efficient. The reasons *f*-CNT is chosen for drug delivery into cancer cells, instead of simple extracellular exposure of drugs, are the control of the solubility [38], long circulating [39], effective crossing of biological barriers [40–42], targeting cancer cells [43–47], efficient drug dosage [16], overcome drug resistance [48], and endosomal escape [49, 50]. Specifically, *f*-CNTs show selective intracellular location [51, 52], proved to be excreted intact [8, 53, 54], and have the capacity of releasing heat upon radiofrequency field that can be used to trigger the drug release mechanism. The stable *f*-CNT drug carrier is able to deliver a payload of drug molecules with much lower degradation kinetics than polymer-based drug delivery systems which suffer poor stability in blood after injection and difficulty in temporally controlling the release of matrix-encapsulated compounds.

The development of the chemistry to open the targeted *f*-CNTs drug carrier is novel. Utilizing this method, the cytotoxics can be stored within the *f*-CNT and have no contact with the outside environment until their release inside the cancer cells. The computational design of the on/off nano-caps based on quantum and molecular dynamics offers accuracy in the structure and energetics of the system, which allows evaluating the time-dosage of the cytotoxics upon pulsed radio frequency radiation. Dual pH/temperature sensitive nano-caps switch on the diffusion of encapsulated cytotoxics into *f*-CNT taking advantage of the CNT property (conversion of the RF absorption into heat) and low pH condition tumor microenvironment.

Approach

This is a preliminary work to the development of a novel self-consistent theoretical–experimental approach. Figure 1 shows the interaction of our theoretical approaches with the knowledge of cancer cell biology and cytotoxics with the purpose of designing the nano-functionalized drug carriers attached to a bispecific scFv antibody in order to encapsulate potent cytotoxics (green zone), which will discriminate cancer cells and avoid side effects of the drugs. The design of all components needs to be engineered using the following techniques:

(1) Quantum mechanical/chemistry calculations that solve the Schrödinger equation to understand and consider effects such as the chemistry and energetics of local interactions [55, 56]. First principles electronic structure techniques have been used recently to understand complex nano-systems in which phenomena at nano-scale affects biological processes difficult to be characterized with macroscopic instrumentation [57–68].
(2) Combined discrete-continuum solutions for electron transfer as a result of the encapsulated cytotoxics and *f*-CNT interaction. Electron transfer process is treated using combined procedures of density functional theory with Green's functions [69–76]. Very important techniques used in energetic materials [77–83] are also needed for the study of cytotoxics.
(3) Molecular mechanics and dynamics methods are used to understand nonlocal and global behavior and to analyze and simulate the whole system [64, 65].

Results of the calculations can also be used to interface quantum and classical mechanics methods trough the force field (FF) parametization. Parameters such as equilibrium bond distances and angles (by optimized structures by QM), bond, angle and dihedral force constants (by vibrational spectra, normal mode calculations with QM), atom charges (ESP charge fitting to reproduce electrostatic potentials of high level QM) and Lennard-Jones parameters (by intermolecular energy fitting with QM).

There is also a need to develop an adequate theory to aid in the drug delivery system design. Usually the computational prediction of the protein-protein binding affinity is not a full atomistic calculation. It is based on solvent accessibility and pair residues potentials, which underestimates the important role of the water and ions in the protein environment. For example, Rosetta's core full atom energy function is a linear sum of molecular mechanics and knowledge-based terms: a 6–12 Lennard-Jones potential, the Lazaridis-Karplus implicit solvation model an explicit hydrogen-bonding potential to describe hydrogen bonding [84].

Calculations should provide important information to build algorithms to design *in silico* an antibody and a smart drug vehicle. The theoretical models can be used to evaluate the affinity, stability and solubility of the engineered bispecific scFv and HER2 receptor (domain IV and II), solubility of the cytotoxic carrier, inertness of the carrier (electron transfer of the carrier and encapsulated cytotoxics), feasibility of opening mechanism of modified drug carrier under external stimuli and its controllable cytotoxics release.

Preliminary work already reported the development of theoretical methods in order to identify the receptor-ligand interaction through ab initio when it involves electron transfer between a receptor and a ligand [85]. This procedure will be scaled up to study interactions among biomolecules such as the interaction between the antibodies and proteins of cancer cells. We have studied the chemistry of structures based on carbon, and our studies showed that the mechanism of the CNT unzipping into graphene is a consequence of the ester bond formation with potassium permanganate [86]. Potassium permanganate breaks bonds far from the ends of the CNT. The unzipped CNTs end-up zigzagged, no matter what was the original chirality as proved experimentally with pristine multiwall carbon nanotubes [87].

Current graphene simulations show that a pristine graphene layer completely encompasses a water droplet and also corroborated [88]. The calculation of binding energy of an encapsulated cytotoxic molecule with CNTs showed that it is energetically feasible to encapsulate cytotoxic drugs into the inner space of a CNT.

The unzipping of the CNT provides a good foundation to implement the required chemistry in the CNT in order to facilitate its opening under cancer cell conditions (lysosomal pH, high oxidant compounds), which supports our proposed technique to encapsulate dissolved cytotoxics in a water droplet in CNT from a graphene.

In order to target the drug delivery system against cancer cells, studies have to focus on the enhancement of affinity of antibodies toward biomolecules that are usually overexpressed in cancer cells, such as epithelial-specific cell adhesion molecule [89, 90], epithelia growth factor receptor [24, 91, 92], vascular endothelial growth factor receptor [93], RAF kinase [94, 95], platelet-derived growth factor [96], $\alpha v\beta 3$ integrins [97], prostate-specific membrane antigens [98], carcinoembryonic antigen-related cell adhesion molecule 6, and ATP- synthase β-subunit [99]. The HER2 receptor target has shown in most studies that HER2-overexpressing occurs predominantly in breast cancer [100]. Trastuzumab and pertuzumab are monoclonal antibodies that inhibit the HER2 activation. HER2 epitopes are different for each antibody; epitope for trastuzumab is on domain IV while that for pertuzumab is on domain II [101].

Cancer cells become trastuzumab resistant within 1 year of treatment initiation because even the HER2 is inactivated and the growth and proliferation downstream signaling pathway could be activated through cross-talk between estrogen receptors and the HER2 [102, 103] as well as the gene mutation events in survival cancer cells [104]. Thus studies propose a treatment based on trastuzumab conjugated with microtubule-depolymerizing agent for avoiding the cancer cell resistance to trastuzumab [105, 106]. In addition, the antibody-receptor mediated internalization is a crucial step for targeted intracellular drug delivery, resulting administration of drugs more efficiently [107]. The fact that antibodies against HER2 receptor are internalized into the cytoplasm when its binding occurs [108–110] suggest their applicability to guide the drug delivery. Besides, this internalization can be accelerated by the addition of a protein (avidin/streptavidin-biotin system) which produces internalization in vitro and in vivo conditions, facilitating the intracellular release of cytotoxins as we propose [111]. In this context, the antibody engineering allows the enhancement of fragment antigen binding (Fab) affinity to antigen [112] and fragment constant (Fc) to Fcγ receptors [113, 114]. In this context, single chain fragment variable (scFv) serves as the basic antigen binding unit to create multispecific molecules [115, 116]. Successful antibody drug conjugates (ADC) development for a given target antigen also depends on the linker stability and mode of linker-drug conjugation to the antibody [117]. To date, one ADC, anti-CD33-calicheamicin conjugate (gemtuzumab ozogamicin or Mylotarg), is approved in the United States for the treatment of acute myeloid leukemia [118].

On other hand, from a clinical perspective, it is important that cancer cells generally are more sensitive to heat induced

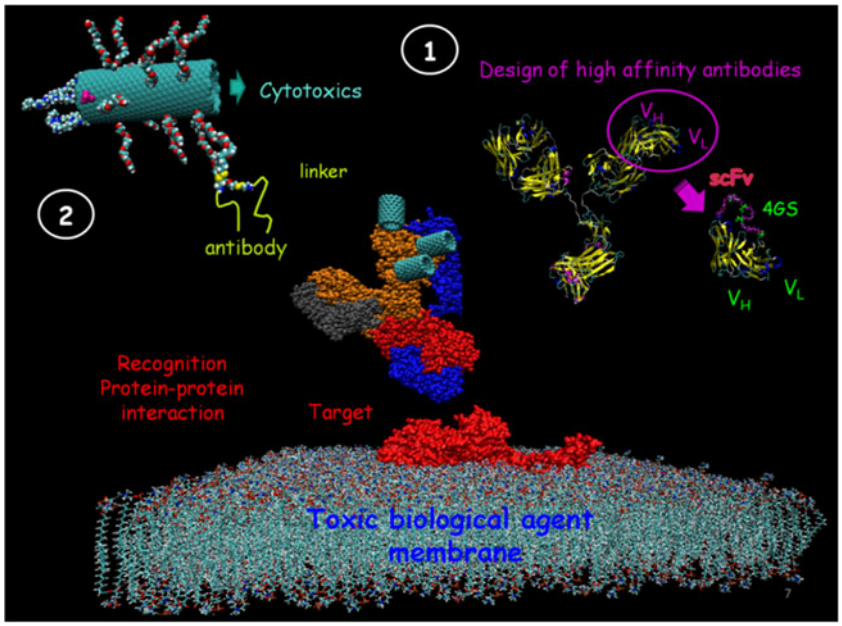

Fig. 2 Mechanism of action of the designed drug delivery systems based on immunoconjugated-CNT against HER2 receptor. (1) Aim1, computational aided design of a high affinity bispecific anti-HER2 antibody based on trastuzumab and pertuzumab Fabs; and (2) Aim2, controllable multiple drug release of the CNT base carrier under external stimuli: opening mechanism

damage and apoptosis than normal cells due to its chronic ischemia, hypoxia and acid pH [119]. Thus, hyperthermia facilitates the cancer cell apoptosis and it acts synergistically to chemotherapy due to its action in chemical reactions involved in cytotoxic modes of action such as doxorubicin, cisplatin, bleomycin, mitomycin, nitrosoureas, cyclophosphamide [120, 121]. In this context, CNT is able to transform the near infrared (NIR) and radio frequency (RF) absorption into heat release; thus it is proposed for non-invasive cancer cell thermal ablation treatment [122]. However, a cancer treatment base on ablation can result in tumor recurrences due to the uncontrollable heterogeneous SWNT concentrations throughout the tumor microenvironment [123]. In addition, the application of CNT for the cancer cell ablation under RF irradiation thermal damage normal liver parenchyma cells in a 3- to 5-mm zone around tumors. Thus, the control of the irradiation is an important issue for avoiding injury to healthy tissue surrounding the treated area.

Figure 2 shows the drug carrier system that allows the HER2/PI3K/Akt/mTOR pathway inhibition by the controllable release of a multi-drug cocktail. This requires understanding the chemistry needed to control the release of those drugs under pulsed RF irradiation in order to develop a sequential drug delivery capacity, such as a multi-drug cocktail consisting of lapanitib (HER2 and HER1 inhibitor) [124], ZSTK474 (PI3k inhibitor), perifosine (Akt inhibitor) and rapamicyn (mTOR inhibitor).

These cytotoxics can be encapsulated into *f*-CNT (Fig. 3) and directed to cancer cells by its conjugation with trastuzumab antibody. The antibody is joined to *f*-CNT based on noncleavable (nonreducible thioether, MCC) linker under a biophysical background that can be summarized with a blood stream with pH 7.35. In addition, the outside of the cancer cell: hypoxia condition, glucose deprivation, high lactate level, extracellular acidosis (around pH 6.5), effect of peroxide in phospholipids and exposure to serum proteins. The endosome/lysosome: ~15 % of the cell volume and pH commonly varies between 4.7 and 5.8 [125]. Irreversible cell damage takes place above 45 °C. On the other hand the size scales are: carrier diameter, 2 nm; antibody, 20 nm; molecule receptor, 20 nm; cell, 10–20 μm; cancer cell membrane thickness, 5 nm; and endosome, 80 nm.

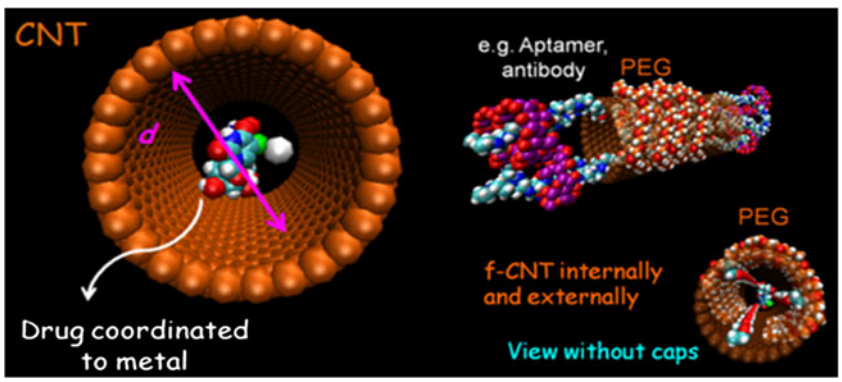

Fig. 3 Encapsulation of a drug molecule into functionalized CNT (*f*-CNT). Design of nanocaps on the CNT edges to block its gaps. The picture shows an external non-covalent functionalization of the CNT with polyethylene glycol (PEG) and internal functionalization with alcohol groups

Results

This study was done in order to consider the computational aided design of a high affinity bispecific anti-HER2 antibody based on trastuzumab and pertuzumab Fabs. Studies show that cancer therapy based on trastuzumab and pertuzumab antibodies block the HER2 receptor synergistically [126]. Therefore, a bispecific single chain fragment variable antibody based on trastuzumab Fab (which recognizes domain IV of HER2) and pertuzumab Fab (which recognize domain II of HER2) can be used, which needs a flexible linker.

Antibody-antigen binding affinity prediction The binding energy of the protein-protein complex is commonly calculated by molecular docking [127–129] or statistical potentials based on the distribution of distances between atoms [130–132]. Furthermore, two characteristics of any protein are considered using molecular dynamics techniques, the flexibility of the binding site and the solvation under physiological environment (ions). They can also be calculated with a full atomistic level by classical molecular dynamics (MD) simulations. Antibody-antigen complexes can be placed in an explicit solvent medium with physiological ion concentration (NaCl=0.145 M). To predict the antibody-ligand complex binding affinity, the solvation energy from the absolute binding free energy calculation is needed. The flexibility of the binding site demands special treatment, for instance, with quantum mechanical approaches to get a better description and thus, force fields for molecular dynamics simulations. Preliminary calculations with the CHARMM force field [133, 134] are performed with the large-scale atomic/molecular massively parallel simulator (LAMMPS) program [135], which includes internal (bonding) terms for bond stretching, angle bending, Urey-Bradley 1,3 interaction, torsional rotation, and out-of-plane (improper) motion while the external (nonbonded) interactions are represented by a Lennard-Jones 6–12 term for the van der Waals repulsion and dispersion interaction, and a Coulomb term for the charge-charge interactions; in the latter both partial and full charges are included. The potential energy function has the form:

$$U\left(\overrightarrow{R}\right) = \sum_{bonds} k_b(b-b_0)^2 + \sum_{angle} k_\theta(\theta-\theta_0)^2 + \sum_{UB} k_{UB}(S-S_0)^2 + \sum_{\text{dihedrals}} \mathrm{k_x}(1+\cos(\mathrm{nx}-\delta)) + \sum_{\text{impropers}} \mathrm{k_{imp}}(\varphi-\varphi_0)^2 + \sum_{\text{nonbond}} \in_{\mathrm{ij}} \left[\left(\frac{\mathrm{R_{min,ij}}}{\mathrm{r_{ij}}}\right)^{12} - 2\left(\frac{\mathrm{R_{min,\,ij}}}{\mathrm{r_{ij}}}\right)^{6}\right] + \frac{\mathrm{q_i q_j}}{4\pi\varepsilon \mathrm{r_{ij}}}$$

where the *ks* are the force constants for the bond (k_b), angle (k_θ), Urey-Bradley 1,3-interaction (k_{UB}), dihedral (k_x), and improper (k_{imp}). The subscript index "0" is the equilibrium value for the bond, angle, Urey-Bradley interaction, and improper. δ is the phase shift, i and j denote two distinct atoms, $\in_{ij}$ is the potential energy minimum between two atoms, and $R_{min,ij}$ is the position of this minimum. ε is the dielectric constant and $\mathrm{q_i}$ are the atomic partial charges.

MD calculations are performed with periodic boundary conditions, preventing water molecules from leaving the system. Constant temperature of the system is maintained at 300 K and 1 atm using the grand-canonical ensemble (NPT).

$$\Delta G_{complex} = \Delta G_{water}(antibody - ligand) - [\Delta G_{water}(antibody) + \Delta G_{water}(ligand)],$$

where

$$\Delta G_{water} = E_{gas} + \Delta G_{solvation} - TS$$
$$G_{solvation} = G_{polar} + G_{nonpolar}$$
$$E_{gas} = E_{internal} + E_{electrostatic} + E_{vdW}$$

and

$$E_{internal} = E_{bond} + E_{angle} + E_{torsion}$$

T is temperature and S entropy. The thermodynamic stability of the wild-type antybody and its mutated trials for maintaining the antibody potency, longer shelf life, longer terminal half-life in vivo and reduced risk of immunogenicity can be evaluated using MD. High thermal stability is essential for tumor targeting of antibody fragments such as single-chain Fv fragment [136]. Thermodynamic stability is evaluated trough the RMSD backbone where an antibody is considered stable if the backbone root-mean-square-deviation is less than 0.5 Å.

Enhanced affinity antibody Fabs: trastuzumab and pertuzumab The algorithms to predict the binding affinity of an antibody-antigen are accurate with the experiment results. The enhancement in the affinity of the antibody variable fragment to different domains of the extracellular portion of HER2 receptor can be performed with MD calculations to identify the "hot spot" residues in Fab fragments that contribute greater to HER2 binding by computational scanning mutagenesis approach. The knowledge of the main interaction between antibody and antigen allows us to enhance its binding affinity. Trastuzumab structure can be based on crystallographic data [137] and also the one for pertuzumab [138]. If antibody structures are not available, they can be

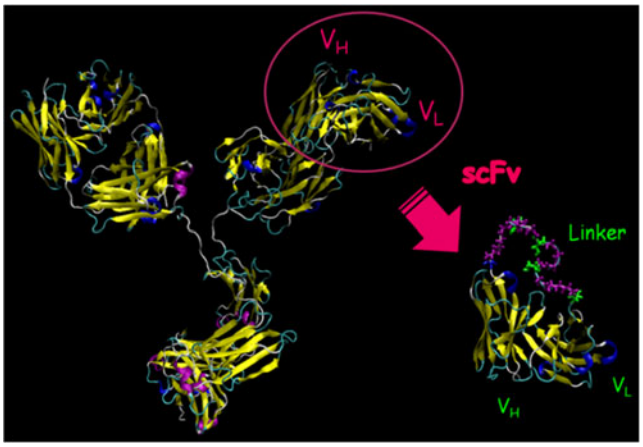

Fig. 4 Single chain variable fragment (scFv) antibody properly selected for the antigen binding site. Variable light and heavy (V_L and V_H) moeities are joined by a polypeptide linker, which permits controlling conjugation of antibody to the CNT

predicted from homologous antibody arrangements and general features of known proteins.

Mutagenesis for improving the affinity of scFvs is based on two types of mutations at antibody-antigen interface: mutation from a hydrophobic amino acid to a larger hydrophobic amino acid, and mutation of partially buried polar groups to a non-polar amino acid considered by increasing of the size of the side-chain. In addition, we will consider mutations that lead to better side-chain packing, hydrogen bonding, and desolvation energies at the interface. Selection of point of mutations does not create large clashes, destabilize the individual chains, or remove key hydrogen bonds across the interface. The free energy of binding of the mutated antibody-antigen complex should be more favorable than the free energy of binding calculated for the wild-type complex over 1.0 kcal mol^{-1} for being considered a positive result.

Our initial test will focus on the relationship between the distribution pattern and the energetic contribution of aromatic residues and interfacial residues (Tyr and Trp). In order to reveal the function of the aromatic residues in the antibody-HER2 binding interface we (1) wild type: compute $\Delta G^{WT}_{complex}$, (2) *in silico* alanine mutations: Tyr and Trp on the binding site, and (3) mutated complex: for the docking simulation, the flexible fitting of ligand within a rigid receptor calculated using the shape-based docking algorithm LigandFit [129]. The best conformation is an indicator of the stability and corresponds to the maximum number and distribution of H-bonding and ionic bonding between the receptor and ligand. This complex can be minimized using molecular mechanics techniques and compute $\Delta G^{WT}_{complex}$ (4) compute $\Delta\Delta G_{binding} = \Delta G^{WT}_{complex} - \Delta G^{WT}_{complex}$. (5) Identify "hot spots" at the interface, and (6) algorithms to determine the adequate mutation in order to increase the affinity of an anti-HER2 antibody.

The above calculations do not take into account changes in conformational entropy, and therefore, the absolute values of the binding energy calculations for a single complex do not represent true free energies. However, changes in binding energy (energy mutant–energy wild-type) do represent

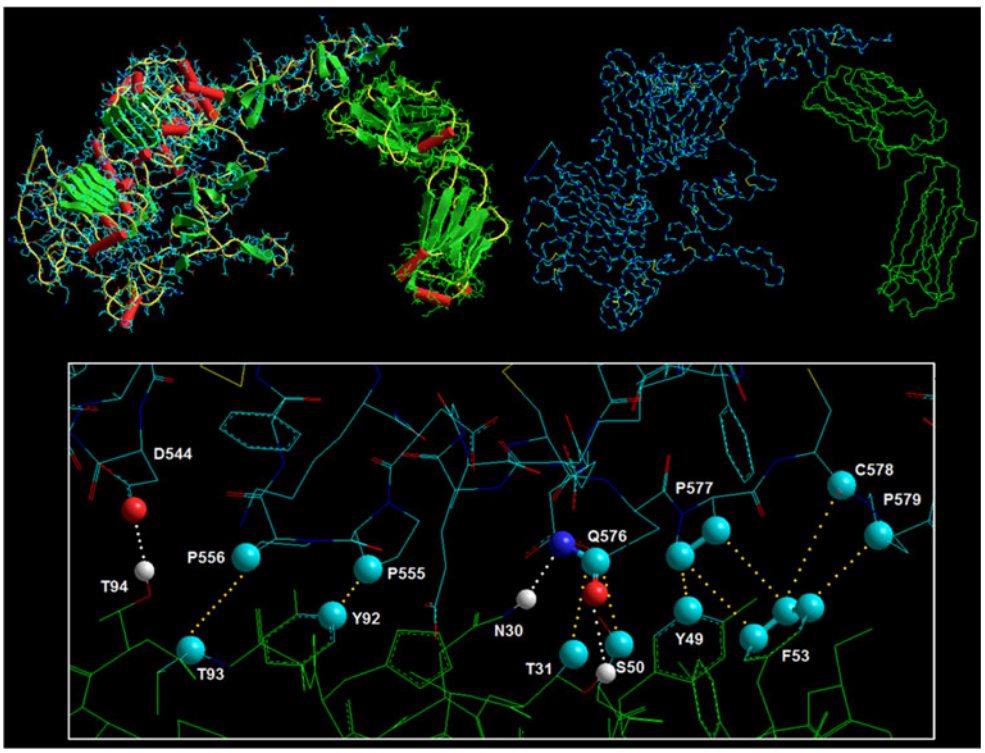

Fig. 5 An example of antigen-antibody complex from crystal data (PDB code 1N8Y and ref. [137]), showing the HER2 (*blue*) complexed with the light chain of Trastuzumab (*green*). The interacting residues of both molecules are depicted at the bottom. *White dashed lines* depict H-bonds (remaining H-atoms are not shown). The hydrophobic van der Waals interactions are more abundant in this region (*yellow dashed lines*)

Table 1 Total energy, dipole moment, highest occupied molecular orbital (HOMO), lowest unoccupied molecular orbital (LUMO) and the gap between the highest occupied and the lowest unoccupied molecular orbital (HLG) of the seven selected drugs for the cancer therapy

Drug		PDB-codes	Energy (Ha)	Dipole (Debye)	HOMO (eV)	LUMO (eV)	HLG (eV)
1	Seliciclib (*R*-roscovitine),	3GGS	−987.18522	3.8463	−6.04	−0.52	5.52
2	Benzimidazole-carboxamide	1EFY	−379.72415	3.486	−6.18	−0.41	5.77
3	Adriamycin/doxorubicin	1D12	−1927.79615	5.797	−5.74	−2.91	2.83
4	Camptothecin	1RR8	−1181.76055	6.394	−6.04	−2.37	3.67
5	Bortezomib	2F16	−1283.45552	8.213	−6.31	−1.33	4.98
6	Imatinib	2PL0	−1581.52536	3.840	−5.47	−2.15	3.32
7	Cytarabine	1P5Z	−890.79182	3.577	−6.15	−0.76	5.39

changes in free energy if one assumes that the conformational entropies of the various states do not change significantly with the mutation.

Design a high affinity bispecific single chain variable fragment (biscFv) antibody (Fig. 4). Commonly, the V_H and V_L fragments are joined by a flexible peptide linker, e.g., (Gly4-Ser)x3 or x4. However, just a linker is not able to avoid the "open form". Thus, we will consider the inclusion of an interchain disulfide bond between V_H and V_L fragments without disturbing the folding and the antigen binding. In this case, we can design an engineered bispecific antibody drug carrier conjugate by noncleavable (nonreducible thioether, MCC) linker activity based on the improved safety profile observed[117]. The proposed linker is bis-maleimido-trioxyethylene glycol (BMPEO) which will be conjugated to cysteine tag (thio-biscFv antibody).

Point mutations can be introduced using the QuickChange® site-directed mutagenesis protocol (Stratagene) and all vectors are verified by DNA sequencing. The method to calculate the K_d of the antibody-ligand complex is the fluorescence polarization binding assay (with thiol reactive bodipy fluorophore) to compare the binding affinities of wild-type with mutated complexes. To evaluate the change in free energy (ΔG) and its component quantities: the change in enthalpy (ΔH) and change in entropy (ΔS), the isothermal titration calorimetry approach [139] can be performed. The ΔG value provides quantification of the affinity of binding between the antibody-antigen interactions.

Present knowledge on antigen-antibody interactions from X-ray crystal structures allow us to analyze the participant atoms in the molecular recognizion between proteins at the borderline antigen-antibody complex. Figure 5 shows an example from the crystal PDB, code 1N8Y [140] of the

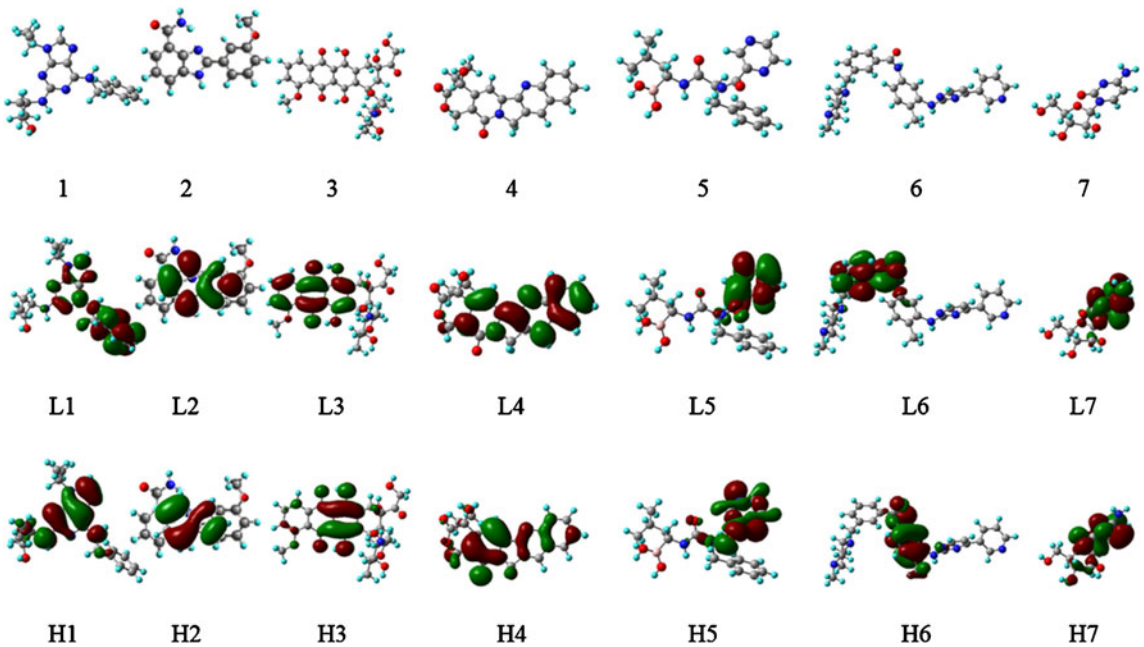

Fig. 6 Optimized structures and frontier molecular orbitals of the seven selected drugs: seliciclib (*R*-roscovitine), benzimidazole-4-carboxamide, doxorubicin, camptothecin, bortezomib, imatinib, and cytarabine. Calculations performed using the B3PW91/6-31G(*d*) level of theory

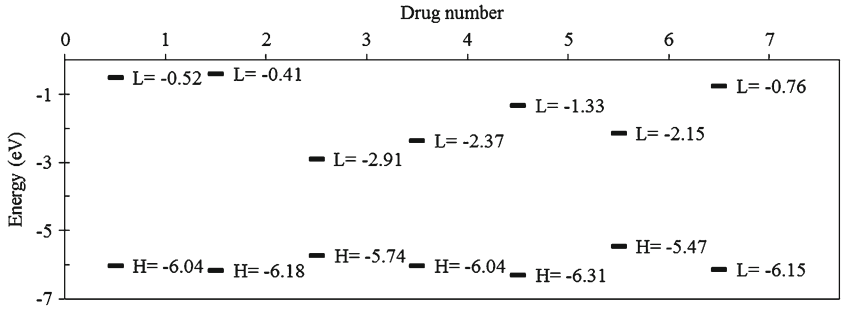

Fig. 7 Plot of lowest unoccupied molecular orbital (L) and highest occupied molecular orbital (H) of seliciclib (drug 1), benzimidazole (drug 2), doxorubicin (drug 3), camptothecin (drug 4), bortezomib (drug 5), imatinib (drug 6) and cytarabine (drug 7). Calculated using the B3PW91/6-31G(*d*) level of theory

group of residues found in contact between the human sHER2 and the light chain of Trastuzumab [137]. Three H-bonds are observed between Asp544-Thr94, Gln576-Asn30 and Gln576-Ser50. A network of hydrophobic contacts are observed as well, where four proline residues (Pro555, 556, 577 and 579), along with Gln576 and Cys578 on the side of the receptor. Thr31 and 93, Tyr49 and 92, Phe53 and Ser50 participate on the side of Trastuzumab. Figure 5 also shows the complex formed by the human sHER2 and the light chain of Trastuzumab.

On the other hand, crystals of seven effective cytotoxics used in cancer therapy, are retrieved from the protein data bank (PDB) and studied at ab initio level theory. Thus, electronic structure and derived properties are assessed as the initial step to conceal the drugs inside the CNT. Along with this, the CNT are built ideally to accept the cytotoxic molecule, leaving at least 4 Å between the drug atoms and the CNT inside wall. Both models, crystal and optimized structures, are studied at B3PW91/6-31G(*d*) level of theory. Table 1 shows names and the electronic properties of the seven drugs, and Fig. 6 show HOMO and LUMO location, and shape of the cytotoxics. These shapes and their energies shown in Table 1 help us to strategically prevent or enhance reactivity with good and bad cell sites, respectively, as well as to predict interactions, electron transfers, steric interactions and stereo-electronics.

The variety of energy values of the HOMO and LUMO among the cytotoxics will allow us to choose the correct match for electron transfer reactions, which are the first interactions after two moieties have recognized each other. In addition, properties such as electron affinity, ionization potential, hardness, and softness can be used properly knowing the target sites of cancer cells. On the other hand, these properties are important to decide the type and size of CNT. Figure 7 reports the energy levels of HOMO and LUMO among the studied drugs. Although HOMO energies are

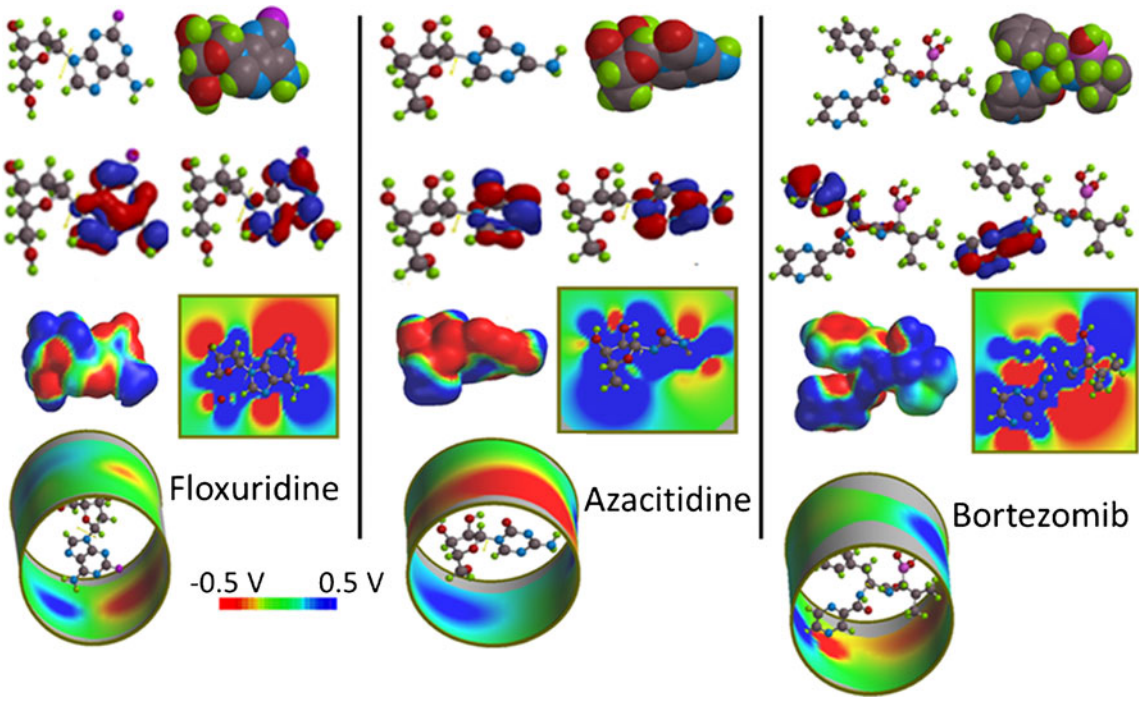

Fig. 8 CPK and ball-stick structures, LUMO and HOMO, and MEPs of floxuridine, azacitidine and bortezomib. These compounds are candidates to be concealed in a CNT. The MEPs are calculated on an isodensity surface, molecular plane and a cylindrical surface. Geometries are from the crystal structure of the compound and MEPs are calculated with the semiempirical Hamiltonian PM3

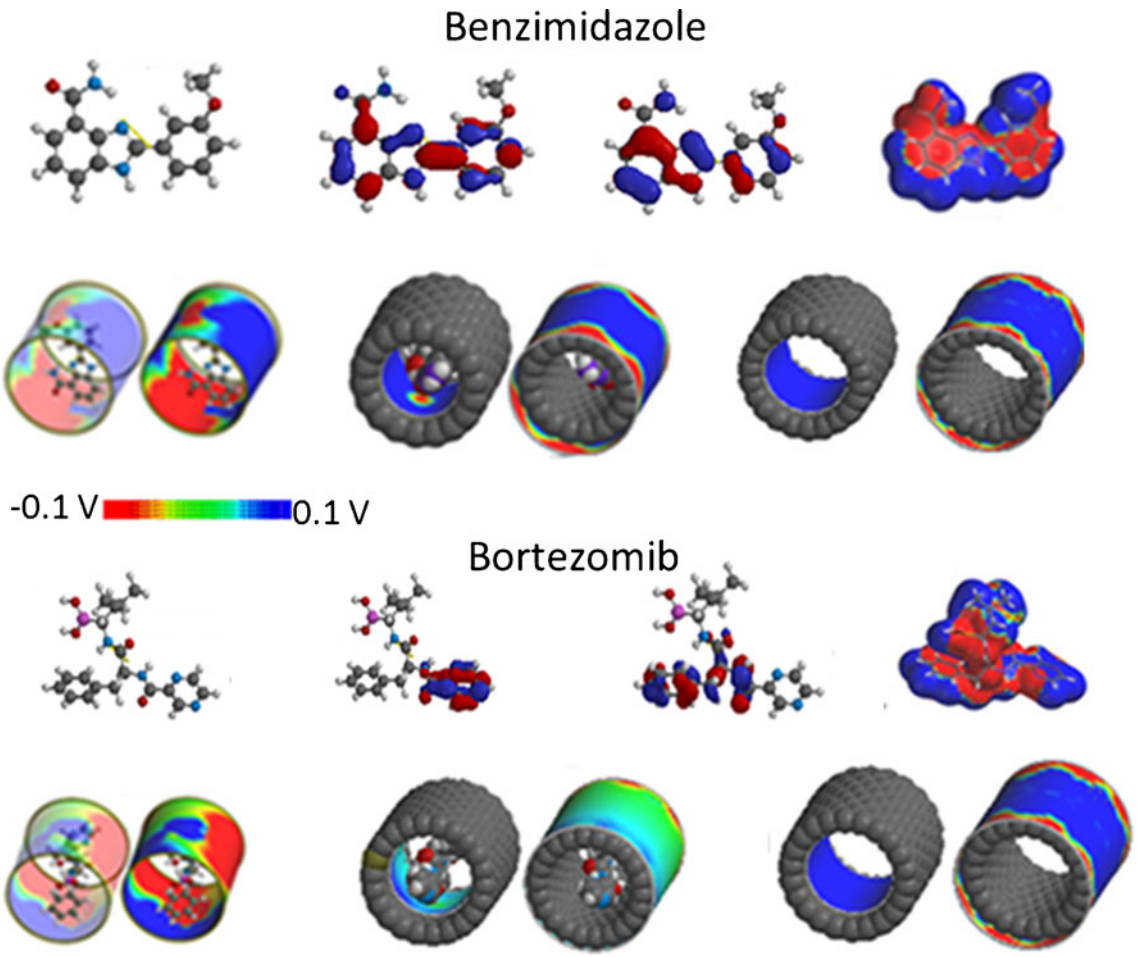

Fig. 9 Geometrical structure, LUMO, HOMO, and MEP of two cytotoxic drugs, benzimidazole and bortezomib, concealed in CNT. The MEPs are plotted on an isodensity surface, cylindrical surface and inside and outside of a CNT. The MEP is color-coded from -0.1 (red) to +0.1 (blue) V

considered acceptable using standard DFT, the LUMO energies still require one more step for their accuracy. This is obtained with time-dependent DFT (TD-DFT).

The molecular electrostatic potential (MEP) shows that the presence of rings reflected in the van der Waals surfaces are similarly represented in the chosen isodensity surfaces. These similarities among the selected molecules also provide a sense of the hydrophobic characteristics of the surface in almost all cases, showing a central positive strip along the molecules. These findings are evident when the MEP is analyzed on cylindrical surroundings of the molecules. The orientation of the molecules is also an important factor for concealing and interacting with the inner face of the CNT. These MEP characteristics are explained for charge distributions and some examples from semiempirical calculations (PM3) are shown in Fig. 8.

The structure and electronic properties of the molecules is followed by the calculation of the size and type of CNT which is studied individually to define its electronic properties and characteristics previous to forming the complex drug-CNT. Figure 9 shows two examples of this procedure with the cytotoxics inside of the CNT.

Conclusions

In summary, we tune the chemistry needed in the caps to develop a viable clinical-therapeutic treatment. The design of this novel drug delivery system will act in a synergistic way among its antibody component, cytotoxics, and induced hyperthermia. Any antibody resistance is overcome by the inhibition of the complete signaling pathway of cell proliferation under hyperthermia condition that can increase the permeability of tumor vasculature, which can enhance the delivery of drugs into tumors. It is important that there are three main critical points that have to be evaluated experimentally: the cytotoxicity of the delivery system, targeting efficiency, and control of the RF irradiation. In addition, calculated parameters can be experimentally validated for obtaining algorithms to allow computational design of a drug delivery system with efficiency.

This work may promote a synergy of techniques and approaches that strongly increases the effectiveness of the fight against cancer by deploying to a target site to limit side

effects, directing antitumoral drugs through specific areas of the body without degradation, maintain a therapeutic drug level for prolonged periods of time, predictable controllable release rates and reduce dosing frequent and increase patient well-being, cure, and healing compliance.

Acknowledgments The authors acknowledge the Texas A&M Supercomputing Facility and the financial support from the U.S. Defense Threat Reduction Agency DTRA through the U.S. Army Research Office, project no. W91NF-06-1-0231, ARO/DURINT project no. W91NF-07-1-0199, and ARO/MURI project no. W911NF-11-1-0024.

References

1. Cui H-F, Vashist SK, Al-Rubeaan K, Luong JHT, Sheu F-S (2010) Interfacing carbon nanotubes with living mammalian cells and cytotoxicity issues. Chem Res Toxicol 23:1131–1147
2. Shen M, Wang SH, Shi X, Chen X, Huang Q, Petersen EJ, Pinto RA, Baker JR Jr, Weber WJ Jr (2009) Polyethyleneimine-mediated functionalization of multiwalled carbon nanotubes: synthesis, characterization, and in vitro toxicity assay. J Phys Chem C 113:3150–3156
3. Kam NWS, Jessop TC, Wender PA, Dai H (2004) Nanotube molecular transporters: internalization of carbon nanotube-protein conjugates into mammalian cells. J Am Chem Soc 126:6850–6851
4. Prato M, Kostarelos K, Bianco A (2009) Functionalized carbon nanotubes in drug design and discovery. Acc Chem Res 41 (1):60–68
5. Ding LH, Stilwell J, Zhang TT, Elboudwarej O, Jiang HJ, Selegue JP, Cooke PA, Gray JW, Chen FQF (2005) Molecular characterization of the cytotoxic mechanism of multiwall carbon nanotubes and nanoonions on human skin fibroblast. Nano Lett 5:2448–2464
6. Pan BF, Cui DX, Xu P, Huang T, Li Q, He R, Gao F (2007) Cellular uptake enhancement of polyamidoamine dendrimer modified single walled carbon nanotube. J Biomed Pharm Eng 1(1):13–16
7. Zhang Y, Bai Y, Yan B (2010) Functionalized carbon nanotubes for potential medicinal applications. Drug Discov Today 15:428–435
8. Kostarelos K, Lacerda L, Pastorin G, Wu W, Wieckowski S, Luangsivilay J, Godefroy S, Pantarotto D, Briand J-P, Muller S, Prato M, Bianco A (2007) Cellular uptake of functionalized carbon nanotubes is independent of functional group and cell type. Nat Nanotechnol 2:108–113
9. Kulamarva A, Bhathena J, Malhotra M, Sebak S, Nalamasu O, Ajayan P, Prakash S (2008) In vitro cytotoxicity of functionalized single walled carbon nanotubes for targeted gene delivery applications. Nanotechnology 2(4):184–188
10. Hwang H, Schatz GC, Ratner MA (2009) Coarse-grained molecular dynamics study of cyclic peptide nanotube insertion into a lipid bilayer. J Phys Chem A 113(16):4780–4787
11. Nielsen SO, Ensing B, Ortiz V, Moore PB, Klein ML (2005) Lipid bilayer perturbations around a transmembrane nanotube: a coarse grain molecular dynamics study. Biophys J 88:3822–3828
12. Raffa V, Ciofani G, Nitodas S, Karachalios T, D'Alessandro D, Masini M, Cuschieri A (2008) Can the properties of carbon nanotubes influence their internalization by living cells? Carbon 46:1600–1610
13. Gao H, Kong Y, Cui D (2003) Spontaneous insertion of DNA oligonucleotides into carbon nanotubes. Nano Lett 3(4):471–473
14. Kam NWS, Dai H (2010) Carbon nanotubes as intracellular protein transporters: generality and biological functionality. JACS 127:6021–6021
15. Liu Z, Fan AC, Rakhra K, Sherlock S, Goodwin A, Chen X, Yang Q, Felsher DW, Dai H (2009) Supramolecular stacking of doxorubicin on carbon nanotubes for in vivo cancer therapy. Angew Chem Int Ed Engl 48:7668–7672
16. Liu Z, Chen K, Davis C, Sherlock S, Cao Q, Chen X, Dai H (2008) Drug delivery with carbon nanotubes for in vivo cancer treatment. Cancer Res 68:6652–6660
17. Li R, Wu R, Zhao L, Wu M, Yang L, Zou H (2010) P-glycoprotein antibody functionalized carbon nanotube overcomes the multidrug resistance of human leukemia cells. ACS Nano 4:1399–1408
18. Chaudhuri P, Soni S, Sengupta S (2010) Single-walled carbon nanotube-conjugated chemotherapy exhibits increased therapeutic index in melanoma. Nanotechnology 21:025102(025101–025110)
19. Zhao D, Alizadeh D, Zhang L, Liu W, Farrukh O, Manuel E, Diamond DJ, Badie B (2010) Carbon nanotubes enhance CpG uptake and potentiate anti-glioma immunity. Clin Cancer Res. doi:10.1158/1078-0432.CCR-10-2444
20. Hampel S, Kunze D, Haase D, Krämer K, Rauschenbach M, Ritschel M, Leonhardt A, Thomas J, Oswald S, Hoffmann V, Büchner B (2008) Carbon nanotubes filled with a chemotherapeutic agent: a nanocarrier mediates inhibition of tumor cell growth. Nanomed 3(2):175–182
21. Marches R, Mikoryak C, Wang R-H, Pantano P, Draper RK, Vitetta ES (2011) The importance of cellular internalization of antibody-targeted carbon nanotubes in the photothermal ablation of breast cancer cells. Nanotechnology 22:95101(95101–95110)
22. Xiao Y, Gao X, Taratula O, Treado S, Urbas A, Holbrook RD, Cavicchi RE, Avedisian CT, Mitra S, Savla R, Wagner PD, Srivastava S, He H (2009) Anti-HER2 IgY antibody-functionalized single-walled carbon nanotubes for detection and selective destruction of breast cancer cells. BMC Cancer 9:351–362
23. Brackstone M, Townson JL, Chambers AF (2007) Tumour dormancy in breast cancer: an update. Breast Cancer Res 9(3):208
24. Al-Nedawi K, Meehan B, Micallef J, Lhotak V, May L, Guha A, Rak J (2008) Intercellular transfer of the oncogenic receptor EGFRvIII by microvesicles derived from tumour cells. Nat Cell Biol 10(5):619–624
25. Pontier SM, Muller WJ (2008) Integrins in breast cancer dormancy. APMIS 116(7–8):677–684
26. Yap X, Tan H-Y, Huang J, Lai Y, Yip GW-C, Tan P-H, Bay B-H (2009) Over-expression of metallothionein predicts chemoresistance in breast cancer. J Pathol 217:563–570
27. Siddik ZH (2006) Cancer drug resistance. In: Teicher BA (ed) Cisplatin resistance, vol III. Humana Press, New Jersey
28. Ciofani G, Raffa V, Menciassi A, Cuschieri A (2009) Boron nitride nanotubes: an innovative tool for nanomedicine. Nano Today 4:8–10
29. Foldvari M, Bagonluri M (2008) Carbon nanotubes as functional excipients for nanomedicines: II. Drug delivery and biocompatibility issues. Nanomedicine: NBM 4(3):183–200
30. Guo BZ, Sadler PJ, Tsang SC (1998) Immobilization and visualization of DNA and proteins on carbon nanotubes. Adv Mater 10 (9):701–703
31. Tripisciano C, Costa S, Kalenczuk RJ, Borowiak-Palen E (2010) Cisplatin filled multiwalled carbon nanotubes - a novel molecular hybrid of anticancer drug container. Eur Biophys J B 75:141–146. doi:10.1140/epjb/e2010-00037-2
32. Heister E, Neves V, Tilmaciu C, Lipert K, Beltran VS, Coley HM, Silvia SRP, McFadden J (2009) Triple functionalisation of single-walled carbon nanotubes with doxorubicin, a monoclonal antibody, and a fluorescent marker for targeted cancer therapy. Carbon 47:2152–2160

33. Cui D, Ozkan CS, Ravindran S, Knog Y, Gao H (2004) Encapsulation of Pt-labelled DNA molecules inside carbon nanotubes. MCB 1(2):113–121
34. Hileman EO, Liu J, Albitar M, Keating MJ, Huang P (2004) Intrinsic oxidative stress in cancer cells: a biochemical basis for therapeutic selectivity. Cancer Chemother Pharmacol 53:209–219
35. Toyokuni S, Okamoto K, Yodoi J, Hiai H (1995) Persistent oxidative stress in cancer. FEBS Lett 358:1–3
36. Szatrowski TP, Nathan CF (1991) Production of large amounts of hydrogen peroxide by human tumor cells. Cancer Res 51:794–798
37. Chiche J, Ilc K, Laferrière J, Trottier E, Dayan F, Mazure NM, Brahimi-Horn MC, Pouysségur J (2009) Hypoxia-inducible carbonic anhydrase IX and XII promote tumor cell growth by counteracting acidosis through the regulation of the intracellular pH. Cancer Res 69:358–368
38. Bianco A, Kostarelos K, Prato M (2008) Opportunities and challenges of carbon-based nanomaterials for cancer therapy. Expert Opin Drug Deliv 5(3):331–342
39. Liu Z, Davis C, Cai W, He L, Chen X, Dai H (2008) Circulation and long-term fate of functionalized, biocompatible single-walled carbon nanotubes in mice probed by Raman spectroscopy. PNAS 105(5):1410–1415
40. Yang Z, Zhang Y, Yang Y, Sun L, Han D, Li H, Wang C (2010) Pharmacological and toxicological target organelles and safe use of single-walled carbon nanotubes as drug carriers in treating Alzheimer disease. Nanomedicine 6(3):427–441
41. Chen X, Schluesener HJ (2010) Multi-walled carbon nanotubes affect drug transport across cell membrane in rat astrocytes. Nanotechnology 21:105104. doi:10.1088/0957-4484/21/10/105104
42. Chaudhuri P, Soni S, Sengupta S (2010) Single-walled carbon nanotube-conjugated chemotherapy exhibits increased therapeutic index in melanoma. Nanotechnology 21:025102 (025111 pp). doi:10.1088/0957-4484/21/2/025102
43. Chen J, Chen S, Zhao X, Kuznetsova LV, Wong SS, Ojima I (2008) Functionalized single-walled carbon nanotube as rationally designed vehicles for tumor-targeted drug delivery. JACS 130:16778–16785
44. Zhang X, Meng L, Lu Q, Fei Z, Dyson PJ (2009) Targeted delivery and controlled release of doxorubicin to cancer cells using modified single wall carbon nanotubes. Biomaterials 30:6041–6047
45. Lay CL, Liu H, Tan H, Liu Y (2010) Delivery of paclitaxel by physically loading onto poly(ethylene glycol) (PEG)-graftcarbon nanotubes for potent cancer therapeutics. Nanotechnology 21:065101 (065110 pp). doi:10.1088/0957-4484/21/6/065101
46. Liu Z, Sun X, Nakayama-Ratchford N, Dai H (2007) Supramolecular chemistry on water-soluble carbon nanotubes for drug loading and delivery. ACS Nano 1(1):50–56
47. Bhirde AA, Patel V, Gavard J, Zhang G, Sousa AA, Masedunskas A, Leapman RD, Weigert R, Gutkind JS, Rusling JF (2009) Targeted killing of cancer cells in vivo and in vitro with EGF-directed carbon nanotube-based drug delivery. ACS Nano 3 (2):307–316
48. Li R, Wu R, Zhao L, Wu M, Yang L, Zou H (2010) P-glycoprotein antibody functionalized carbon nanotube overcomes the multidrug resistance of human leukemia cells. ACS Nano 4(3):1399–1408. doi:10.1021/nn9011225
49. Kam NWS, Liu Z, Dai H (2005) Functionalization of carbon nanotubes via cleavable disulfide bonds for efficient intracellular delivery of siRNA and potent gene silencing. JACS 127:12492–12493
50. Mu Q, Broughton DL, Yan B (2009) Endosomal leakage and nuclear translocation of multiwalled carbon nanotubes: developing a model for cell uptake. Nano Lett 9(12):4370–4375
51. Firme CP III, Bandaru PR (2010) Toxicity issues in the application of carbon nanotubes to biological systems. Nanomedicine: NBM 6:245–256
52. Krajcik R, Jung A, Hirsch A, Neuhuber W, Zolk O (2008) Functionalization of carbon nanotubes enables non-covalent binding and intracellular delivery of small interering RNA for efficient knock-down of genes. Biochem Biophys Res Commun 369:595–602
53. Dumortier H, Lacotte S, Pastorin G, Marega R, Wu W, Bonifazi D, Briand J-P, Prato M, Muller S, Bianco A (2006) Functionalized carbon nanotubes are non-cytotoxic and preserve the functionality of primary immune cells. Nano Lett 6(7):1522–1528
54. Singh R, Pantarotto D, Lacerda L, Pastorin G, Klumpp C, Prato M, Bianco A, Kostarelos K (2006) Tissue biodistribution and blood clearance rates of intravenously administered carbon nanotube radiotracers. PNAS 103(9):3357–3362
55. Hohenberg P, Kohn W (1964) Inhomogeneous electron gas. Phys Rev 136(3B):B864
56. Kohn W, Sham LJ (1965) Self-consistent equations including exchange and correlation effects. Phys Rev 140(4A):A1133
57. Balbuena PB, Altomare D, Agapito LA, Seminario JM (2003) Theoretical analysis of oxygen adsorption on Pt-based clusters alloyed with Co, Ni, or Cr embedded in a Pt matrix. J Phys Chem B 107(49):13671–13680
58. Derosa PA, Seminario JM, Balbuena PB (2001) Properties of small bimetallic Ni-Cu clusters. J Phys Chem A 105(33):7917–7925
59. Zacarias AG, Castro M, Tour JM, Seminario JM (1999) Lowest energy states of small Pd clusters using density functional theory and standard ab initio methods. A route to understanding metallic nanoprobes. J Phys Chem A 103(38):7692–7700
60. Seminario JM, Zacarias AG, Castro M (1997) Systematic study of the lowest energy states of Pd, Pd_2, and Pd_3. Int J Quantum Chem 61:515–523
61. Seminario JM, Agapito LA, Yan L, Balbuena PB (2005) Density functional theory study of adsorption of OOH on Pt-based bimetallic clusters alloyed with Cr, Co, and Ni. Chem Phys Lett 410(4–6):275–281
62. Seminario JM, Tour JM (1997) Systematic study of the lowest energy states of Au_n (n=1−4) using DFT. Int J Quantum Chem 65:749–758
63. Seminario JM, Ma Y, Agapito LA, Yan L, Araujo RA, Bingi S, Vadlamani NS, Chagarlamudi K, Sudarshan TS, Myrick ML, Colavita PE, Franzon PD, Nackashi DP, Cheng L, Yao Y, Tour JM (2004) Clustering effects on discontinuous gold film nanoCells. J Nanosci Nanotechnol 4(7):907–917
64. Seminario JM, Concha MC, Politzer P (1995) A density functional/molecular dynamics of the structure of liquid nitromethane. J Chem Phys 102(20):8281–8282
65. Seminario JM, Concha MC, Murray JS, Politzer P (1994) Theoretical analyses of O_2/H_2O systems under normal and supercritical conditions. Chem Phys Lett 222(1–2):25–32
66. Politzer P, Seminario J, Bolduc P (1989) A proposed interpretation of the destabilizing effect of hydroxyl-groups on nitroaromatic molecules. Chem Phys Lett 158(5):463–469
67. Murray J, Redfern P, Seminario J, Politzer P (1990) Anomalous energy effects in some aliphatic and alicyclic Aza systems and their nitro-derivatives. J Phys Chem 94(6):2320–2323
68. Murray JS, Seminario JM, Politzer P (1994) Does antiaromaticity imply Net destabilization. Int J Quantum Chem 49(5):575–579
69. Nel AE, Madler L, Velegol D, Xia T, Hoek EMV, Somasundaran P, Klaessig F, Castranova V, Thompson M (2009) Understanding biophysicochemical interactions at the nano-bio interface. Nat Mater 8(7):543–557
70. Seminario JM, Yan L (2005) Ab initio analysis of electron currents in thioalkanes. Int J Quantum Chem 102:711–723

71. Derosa PA, Guda S, Seminario JM (2003) A programmable molecular diode driven by charge-induced conformational changes. J Am Chem Soc 125:14240–14241
72. Seminario JM, De La Cruz C, Derosa PA, Yan L (2004) Nanometer-size conducting and insulating molecular devices. J Phys Chem B 108(46):17879–17885
73. Seminario JM, Araujo RA, Yan L (2004) Negative differential resistance in metallic and semiconducting clusters. J Phys Chem B 108(22):6915–6918
74. Seminario JM, Derosa PA, Cordova LE, Bozard BH (2004) A molecular device operating at terahertz frequencies. IEEE Trans Nanotechnol 3(1):215–218
75. Seminario JM, Yan L, Ma Y (2005) Scenarios for molecular-level signal processing. Proc IEEE 93(10):1753–1764
76. Seminario JM, Sanders FC (1990) Application of Z-dependent perturbation-theory to autoionizing states of HeliumLike atoms–feshbach projection method. Phys Rev A 42(5):2562–2572
77. Grodzicki M, Seminario JM, Politzer P (1991) Energy barriers of symmetry-forbidden reactions: local density functional calculations. J Chem Phys 94(2):1668–1669
78. Politzer P, Seminario JM (1989) Computational determination of the structures and some properties of tetrahedrane, prismane, and some of their Aza analogues. J Phys Chem 93:588–592
79. Habibollahzadeh D, Grodzicki M, Seminario JM, Politzer P (1991) Computational study of the concerted gas-phase triple dissociations of 1,3,5-triazacyclohexane and its 1,3,5-trinitro derivative (RDX). J Phys Chem 95:7699–7702
80. Politzer P, Seminario JM (1993) Computational study of the structure of dinitraminic acid, $HN(NO_2)_2$ and the energetics of some possible decomposition steps. Chem Phys Lett 216:348–352
81. Politzer P, Seminario JM (1993) Energy changes associated with some decomposition steps of 1,3,3-trinitroazetidine - a nonlocal density-functional study. Chem Phys Lett 207(1):27–30
82. Seminario JM, Concha MC, Politzer P (1992) Calculated structures and relative stabilities of furoxan, some 1,2 dinitrosoethylenes and other isomers. J Comput Chem 13(2):177–182
83. Choi D-S, Huang S, Huang M, Barnard TS, Adams RD, Seminario JM, Tour JM (1998) Revised structures of N-substituted dibrominated pyrrole derivatives and their polymeric products. Termaleimide models with Low optical bandgaps. J Org Chem 63(8):2646–2655
84. Meiler J, Baker D (2006) ROSETTALIGANDS: protein-small molecules docking with full side-chain flexibility. Proteins Struct Funct Bioinformatics 65:538–548
85. Salazar PF, Seminario JM (2008) Identifying receptor-ligand interactions through an ab initio approach. J Phys Chem B 112 (4):1290–1292. doi:doi:10.1021/jp0768569
86. Rangel NL, Sotelo JC, Seminario JM (2010) Mechanism of carbon nanotubes unzipping into graphene ribbons. J Chem Phys 131:031105(031101–031104)
87. Kosynkin DV, Higginbotham AL, Sinitskii A, Lomeda JR, Dimiev A, Price BK, Tour JM (2009) Longitudinal unzipping of carbon nanotubes to form graphene nanoribbons. Nature 458:872–876
88. Niladri Patra BW, Krlál P (2009) Nanodroplet activated and guided folding of graphene nanostructures. Nano Lett 9 (11):3766–3771
89. Carpenter G, Brewer MR (2009) EpCAM: another surface-to-nucleus missile. Cancer Cell 15:165–166
90. Hussain S, Plückthun A, Allen TM, Zangemeister-Wittke U (2007) Antitumor activity of an epithelial cell adhesion molecule–targeted nanovesicular drug delivery system. Mol Cancer Ther 6(11):3019–3027
91. Hynes NE, Lane HA (2005) ErbB receptors and cancer: the complexity of targeted inhibitors. Nat Rev 5:341–354
92. Kuan C-T, Wikstrand CJ, Bigner DD (2001) EGF mutant receptor vIII as a molecular target in cancer therapy. Endocr Relat Cancer 8:83–96
93. Hicklin DJ, Ellis LM (2005) Role of the vascular endothelial growth factor pathway in tumor growth and angiogenesis. J Clin Oncol 23:1011–1027
94. Gollob JA, Wilhelm S, Carter C, Kelley SL (2006) Role of Raf kinase in cancer: therapeutic potential of targeting the Raf/MEK/ERK signal transduction pathway. Semin Oncol 33(4):392–406
95. Strumberg D, Richly H, Hilger RA, Schleucher N, Korfee S, Tewes M, Faghih M, Brendel E, Voliotis D, Haase CG, Schwartz B, Awada A, Voigtmann R, Scheulen ME, Seeber S (2005) Phase I clinical and pharmacokinetic study of the novel Raf kinase and vascular endothelial growth factor receptor inhibitor BAY 43–9006 in patients with advanced refractory solid tumors. J Clin Oncol 23(5):965–972
96. Polyzos A (2008) Activity of SU11248, a multitargeted inhibitor of vascular endothelial growth factor receptor and platelet-derived growth factor receptor, in patients with metastatic renal cell carcinoma and various other solid tumors. j steroid biochem mol biol 108(3–5):261–266
97. Nasongkla N, Bey E, Ren J, Ai H, Khemtong C, Guthi JS, Chin S-F, Sherry AD, Boothman DA, Gao J (2006) Multifunctional polymeric micelles as cancer-targeted, MRI-ultrasensitive drug delivery systems. Nano Lett 6(11):2427–2430
98. Kim E, Jung Y, Choi H, Yang J, Suh J-S, Huh Y-M, Kim K, Haam S (2010) Prostate cancer cell death produced by the co-delivery of Bcl-xL shRNA and doxorubicin using an aptamer-conjugated polyplex. Biomaterials In Press, Corrected Proof. doi:10.1016/j.biomaterials.2010.02.030
99. Huang T-C, Chang H-Y, Hsu C-H, Kuo W-H, Chang K-J, Juan H-F (2008) Targeting therapy for breast carcinoma by ATP synthase inhibitor aurovertin B. J Proteome Res 7(4):1433–1444
100. Arribas J, Parra-Palau JL, Pedersen K (2010) HER2 Fragmentation and breast cancer stratification. Clin Cancer Res 16(16):4071–4073
101. Fisher RD, Ultsch M, Lingel A, Schaefer G, Shao L, Birtalan S, Sidhu SS, Eigenbrot C (2010) Structure of the complex between HER2 and an antibody paratope formed by side chains from tryptophan and serine. J Mol Biol 402:217–229
102. Nahta R, Yu D, Hung M-C, Hortobagyi GN, Esteva FJ (2006) Mechanisms of disease: understanding resistance to HER2-targeted therapy in human breast cancer. Nature 3(5):269–280
103. Longva KE, Pedersen NM, Haslekas C, Stang E, Madshus IH (2005) Herceptin-induced inhibition of ErbB2 signaling involves reduced phosphorylation of Akt but not endocytic down-regulation of ErbB2. Int J Cancer 116:359–367
104. Ono M, Kuwano M (2006) Molecular mechanisms of epidermal growth factor receptor (EGFR) activationand response to gefitinib and other EGFR-targeting drugs activationand response to gefitinib and other EGFR-targeting drugs. Clin Cancer Res 12:7242–7251
105. Barginear MF, Budman DR (2009) Trastuzumab-DM1: a review of the novel immuno-conjugate for HER2-overexpressing breast cancer. Open Breast Cancer J 1:25–30
106. Mamot C, Drummond DC, Greiser U, Hong K, Kirpotin DB, Marks JD, Park JW (2003) Epidermal growth factor receptor (EGFR)-targeted immunoliposomes mediate specific and efficient drug delivery to EGFR- and EGFRvIII-overexpressing tumor cells. Cancer Res 63:3154–3161
107. Wu AM, Senter PD (2005) Arming antibodies: prospects and challenges for immunoconjugates. Nat Biotechnol 23:1137–1146
108. Roepstorff K, Grøvdal L, Grandal M, Lerdrup M, Deurs B (2008) Endocytic downregulation of ErbB receptors: mechanisms and relevance in cancer. Histochem Cell Biol 129:563–578

109. Ben-Kasus T, Schechter B, Lavi S, Yarden Y, Sela M (2008) Persistent elimination of ErbB-2/HER2-overexpressing tumors using combinations of monoclonal antibodies: relevance of receptor endocytosis. PNAS 106(9):3294–3299
110. Austin CD, Mazière AMD, Pisacane PI, Dijk SM, Eigenbrot C, Sliwkowski MX, Klumperman J, Scheller RH (2004) Endocytosis and sorting of ErbB2 and the site of action of cancer therapeutics trastuzumab and geldanamycin. Mol Biol Cell 15:5268–5282
111. Zhu W, Okollie B, Artemov D (2007) Controlled internalization of Her-2/neu receptors by cross-linking for targeted delivery. Cancer Biol Ther 6:1960–1966
112. Baer M, Sawa T, Flynn P, Luehrsen K, Martinez D, Wiener-Kronish JP, Yarranton G, Bebbington C (2009) An engineered human antibody Fab fragment specific for *pseudomonas aeruginosa* PcrV antigen Has potent antibacterial activity. Infect Immun 77:1083–1090
113. Schlaeth M, Berger S, Derer S, Klausz K, Lohse S, Dechant M, Lazar GA, Schneider-Merck T, Peipp M, Valerius T Fc-engineered EGF-R antibodies mediate improved antibody-dependent cellular cytotoxicity (ADCC) against KRAS-mutated tumor cells. Cancer Science 101 (5):1080–1088. doi:10.1111/j.1349-7006.2010.01505.x
114. Zalevsky J, Leung IWL, Karki S, Chu SY, Zhukovsky EA, Desjarlais JR, Carmichael DF, Lawrence CE (2009) The impact of Fc engineering on an anti-CD19 antibody: increased Fcγ receptor affinity enhances B-cell clearing in nonhuman primates. Blood 113:3735–3743
115. Weisser NE, Hall JC (2009) Applications of single-chain variable fragment antibodies in therapeutics and diagnostics. Biotechnol Adv 27:502–520
116. Orcutt KD, Ackerman ME, Cieslewicz M, Quiroz E, Slusarczyk AL, Frangioni JV, Wittrup KD (2010) A modular IgG-scFv bispecific antibody topology. Protein Eng Des Sel 23:221–228
117. Junutula JR, Flagella KM, Graham RA, Parsons KL, Ha E, Raab H, Bhakta S, Nguyen T, Dugger DL, Li G, Mai E, Phillips GDL, Hiraragi H, Fuji RN, Tibbitts J, Vandlen R, Spencer SD, Scheller RH, Polakis P, Sliwkowski MX (2010) Engineered thio-trastuzumab-DM1 conjugate with an improved therapeutic index to target human epidermal growth factor receptor 2–positive breast cancer. Clin Cancer Res 16:4769–4778
118. Naito K, Takeshita A, Shigeno K, Nakamura S, Fujisawa S, Shinjo K, Yoshida H, Ohnishi K, Mori M, Terakawa S, Ohno R (2000) Calicheamicin-conjugated humanized anti-CD33 monoclonal antibody (gemtuzumab zogamicin, CMA-676) shows cytocidal effect on CD33-positive leukemia cell lines, but is inactive on P-glycoprotein-expressing sublines. Leukemia 14:1436–1443
119. Palazzi M, Maluta S, Dall'Oglio S, Romano M (2010) The role of hyperthermia in the battle against cancer. Tumori 96:902–910
120. Takahashi I, Emi Y, Hasuda S, Kakeji Y, Maehara Y, Sugimachi K (2002) Clinical application of hyperthermia combined with anticancer drugs for the treatment of solid tumors. Surgery 131 (1, Supplement 1):S78–S84
121. Nakao K, Otsuki Y, Akao Y, Ito Y, Marukawa O, Tachibana S, Kawakami M, Sasaki S (2000) The synergistic effects of hyperthermia and anticancer drugs on induction of apoptosis. Med Electron Microsc 33(1):44–50. doi:10.1007/s007950000007
122. Moon HK, Lee SH, Choi HC (2009) In vivo near-infrared mediated tumor destruction by photothermal effect of carbon nanotubes. ACS Nano 3(11):3707–3713
123. Gannon CJ, Cherukuri P, Yakobson BI, Cognet L, Kanzius JS, Kittrell C, Weisman RB, Pasquali M, Schmidt HK, Smalley RE, Curley SA (2007) Carbon nanotube-enhanced thermal destruction of cancer cells in a noninvasive radiofrequency field. Cancer 110(12):2654–2665. doi:10.1002/cncr.23155
124. Cameron DA, Stein S (2008) Drug insight: intracellular inhibitors of HER2[mdash]clinical development of lapatinib in breast cancer. Nat Clin Prac Oncol 5(9):512–520
125. Lee RJ, Wang S, Low PS (1995) Measurement of endosome pH following folate receptor-mediated endocytosis. Biochim Biophys Acta, Mol Cell Res 1312(3):237–242
126. Nahta R, Hung M-C, Esteva FJ (2004) The HER-2-targeting antibodies trastuzumab and pertuzumab synergistically inhibit the survival of breast cancer cells. Cancer Res 64:2343–2346
127. Böhm H-J (1992) The computer program LUDI: a new method for the de novo design of enzyme inhibitors. J Comput Aided Mol Des 6(1):61–78
128. Rarey M, Wefing S, Lengauer T (1996) Placement of medium-sized molecular fragments into active sites of proteins. J Comput Aided Mol Des 10(1):41–54
129. Venkatachalam CM, Jiang X, Oldfield T, Waldman M (2003) LigandFit: a novel method for the shape-directed rapid docking of ligands to protein active sites. J Mol Graph Model 21(4):289–307
130. Cramer CJ, Truhlar DG (1999) Implicit solvation models: equilibria, structure, spectra, and dynamics. Chem Rev 99(8):2161–2200
131. Gehlhaar DK, Verkhivker GM, Rejto PA, Sherman CJ, Fogel DR, Fogel LJ, Freer ST (1995) Molecular recognition of the inhibitor AG-1343 by HIV-1 protease: conformationally flexible docking by evolutionary programming. Chem Biol 2(5):317–324
132. Muegge I, Martin YC (1999) A general and fast scoring function for protein-ligand interactions: a simplified potential approach. J Med Chem 42(5):791–804
133. Brooks BR, Bruccoleri RE, Olafson BD, States DJ, Swaminathan S, Karplus M (1983) CHARMM: a program for macromolecular energy, minimization, and dynamics calculations. J Comput Chem 4(2):187–217
134. Alexander D, MacKerell J, Wi rkiewicz-Kuczera J, Karplus M (1995) An All-atom empirical energy function for the simulation of nucleic acids. J Am Chem Soc 117:11946–11975
135. Plimpton SJ (1997) Fast parallel algorithms for short-range molecular dynamics. J Comp Phys 117:1–19
136. Miller BR, Demarest SJ, Lugovskoy A, Huang F, Wu X, Snyder WB, Croner LJ, Wang N, Amatucci A, Michaelson JS, Glaser SM (2010) Stability engineering of scFvs for the development of bispecific and multivalent antibodies. Protein Eng Des Sel 23:549–557
137. Cho H-S, Mason K, Ramyar KX, Stanley AM, Gabelli SB, Denney DW Jr, Leahy DJ (2003) Structure of the extracellular region of HER2 alone and in complex with the Herceptin Fab. Nature 421:756–760
138. Franklin MC, Carey KD, Vajdos FF, Leahy DJ, de Vos AM, Sliwkowski MX (2004) Insights into ErbB signaling from the structure of the ErbB2-pertuzumab complex. Cancer Cell 5:317–328
139. Olsson TSG, Williams MA, Pitt WR, Ladbury JE (2008) The thermodynamics of protein-ligand interaction and solvation: insights for ligand design. J Mol Biol 384(4):1002–1017
140. Bernstein FC, Koetzle TF, Williams GJ, Meyer EE, Brice MD, Rodgers JR, Kennard O, Shimanouchi T, Tasumi M (1997) The protein data bank. J Mol Biol 112:535–542